




## Article

# Investigation of Puffing and Micro-Explosion of Water-in-Diesel Emulsion Spray Using Shadow Imaging

Mhadi A. Ismael <sup>1,\*</sup>, Morgan R. Heikal <sup>1,2</sup>, A. Rashid A. Aziz <sup>1,\*</sup>, Cyril Crua <sup>2</sup> ,  
Mohammed El-Adawy <sup>1</sup> , Zuhaib Nissar <sup>1</sup>, Masri B. Baharom <sup>1</sup>, Ezrann Z. Zainal A. <sup>1</sup> and  
Firmansyah <sup>1</sup> 

<sup>1</sup> Mechanical Engineering Department, Universiti Teknologi Petronas, Seri Iskandar 32610, Malaysia; M.R.Heikal@brighton.ac.uk (M.R.H.); engmohammed\_2008@yahoo.com (M.E.-A.); zuhaib\_16000073@utp.edu.my (Z.N.); masrib@utp.edu.my (M.B.B.); ezrann.zainal@utp.edu.my (E.Z.Z.A.); firmansyah@utp.edu.my (F.)

<sup>2</sup> School of Computing Engineering and Mathematics, University of Brighton, Brighton BN2 4GJ, UK; c.crua@brighton.ac.uk

\* Correspondence: xmhadosx@yahoo.com (M.A.I.); rashid@utp.edu.my (A.R.A.A.); Tel.: +60-05-373-1507 (M.A.I.); +60-05-368-8104 (A.R.A.A.)

Received: 11 July 2018; Accepted: 1 August 2018; Published: 30 August 2018



**Abstract:** Water-in-diesel emulsions potentially favor the occurrence of micro-explosions when exposed to elevated temperatures, thereby improving the mixing of fuels with the ambient gas. The distributions and sizes of both spray and dispersed water droplets have a significant effect on puffing and micro-explosion behavior. Although the injection pressure is likely to alter the properties of emulsions, this effect on the spray flow puffing and micro-explosion has not been reported. To investigate this, we injected a fuel spray using a microsyringe needle into a high-temperature environment to investigate the droplets' behavior. Injection pressures were varied at 10%  $v/v$  water content, the samples were imaged using a digital microscope, and the dispersed droplet size distributions were extracted using a purpose-built image processing algorithm. A high-speed camera coupled with a long-distance microscope objective was then used to capture the emulsion spray droplets. Our measurements indicated that the secondary atomization was significantly affected by the injection pressure which reduced the dispersed droplet size and hence caused a delay in puffing. At high injection pressure (500, 1000, and 1500 bar), the water was evaporated during the spray and although there was not enough droplet residence time, puffing and micro-explosion were clearly observed. This study suggests that high injection pressures have a detrimental effect on the secondary atomization of water-in-diesel emulsions.

**Keywords:** water-in-diesel; micro-explosion; puffing; dispersed water droplet

## 1. Introduction

Admission of water into diesel engines can play a significant role in the simultaneous reduction of nitrogen oxides (NO<sub>x</sub>) and particulate matter (PM) [1]. Different methods have been proposed to classify the use of water in the engine cylinder, including through injection into the intake manifold [2], an injection of water into the cylinder [3,4], and emulsification of water and diesel prior to injection into the chamber [5,6]. However, there is a growing body of literature that recognizes the presence of water as emulsified diesel fuel reduces harmful emissions, while simultaneously improving the combustion process. Emulsion is formed from immiscible liquids, the oil (continuous phase) and water droplets (disperse phase) being tied together with the aid of chemical additives—so-called

surfactants [7]. With water-in-diesel emulsion, the vaporization of water during the spray causes a reduction of NO<sub>x</sub> emission [8], while secondary atomization improves the combustion process due to better air-fuel mixing [9]. For the secondary atomization of emulsions, both micro-explosion and puffing are the key factors that influence the fuel mixing process. Micro-explosion is when droplets burst into smaller droplets due to explosive boiling of the dispersed water inside a continuous oil phase (immiscibility and different volatility of the two liquid components) which causes the disruption of the parent drops and, hence, a secondary atomization. Puffing is when water droplets (or vapor) erupt from the surface of the parent droplet without its complete breakup.

Different experiments have been conducted using water-in-diesel emulsion of an engine fuel and explained the combustion and micro-explosion processes. An increase of macroscopic spray dispersion angle and spray tip penetration are often used to describe the micro-explosion phenomena [10]. An observation of longer ignition delay [11,12] and shorter combustion duration also featured in micro-explosions and, hence, promoted the combustion [13]. Direct visualization techniques captured the explosions of small droplets in the spray flame [14], and glowing spots, due to disruption of the droplet [15], were also used to describe the micro-explosion phenomena. It should be noted that micro-explosion is a quick event which cannot be visualized easily at engine operating conditions; hence, single-droplet experiments were often used to facilitate the observation of the fast evaporation of the droplet, and thus develop hypotheses on the performance of emulsions in engines [16–19].

A considerable amount of literature has been published on micro-explosion and puffing using single-droplet experiments [18,20–24]. These studies have confirmed that large isolated droplets of emulsified fuel lead to puffing and/or micro-explosion, with their occurrences depending on several factors. The coalescence and phase separation of emulsions are among the most important factors. Other factors include the type and amount of surfactant, water content in the emulsion and the size of the dispersed water droplets. A higher surfactant content was found to delay the micro-explosion occurrences [17], while, in contrast, the increase of water content in the emulsion was found to decrease the emulsion stability and enhance the intensity of micro-explosion [25]. The optimum water concentration in the emulsion was found to be 10% [26]. The intensity of micro-explosion was found to be higher with dispersed water droplet sizes larger than 10  $\mu\text{m}$  [27]. However, with a reduction in the dispersed water droplets size to 2  $\mu\text{m}$ , the temperature required for micro-explosion increased [28]. The dispersed droplet size was functioning optimally at 4.7  $\mu\text{m}$  [29]. The increase in the breakup rate caused by mechanical stirrers results in smaller droplet sizes [27], whilst in larger droplet sizes, the coalescence rate of dispersed phase increased [30].

Recent studies demonstrated a strong and consistent association between the water content, dispersed water droplet size, and temperature [31]. Therefore, to control the secondary atomization of water-in-diesel emulsion it is essential to control the sizes and numbers of the dispersed phase. It should be noted that the emerging emulsions from the injector nozzle are significantly different compared with the unused fuel in the tank [32]. We recently investigated the impact of fuel pump and injector nozzle on the dispersed water droplet size and found that the emulsions were subjected to intense shear in the fuel pump and injector nozzle which led to change in the distributions and sizes of the emulsion droplets [32]. These results also showed that the water content in the emulsion was significantly reduced after passing the injection equipment.

In single suspended droplet experiments the onset of the micro-explosion phenomena was found to be affected by the size of the parent droplet. In these experiments the droplet diameters ranged from 1 to 2 mm. The droplets were either suspended on a wire above the hot plate using a fiber-supported technique or were made to free fall. If the wire is used, micro-explosion is caused by not only nucleation inside the droplet but also by the effect of the wire's surface [33]. Therefore, some studies used unsupported techniques to reduce experimental uncertainty. However, these studies used relatively large droplet sizes ranging from 200 to 1000  $\mu\text{m}$ , whilst realistic spray droplet sizes are below 100  $\mu\text{m}$ . In fact, in a large droplet size, the droplet heating and waiting time was found to affect the strength of micro-explosion [34]. Therefore, several interesting questions remain about

the consistence of the relationship between the initial and dispersed water droplets on puffing and or micro-explosion phenomena.

This article begins by describing the emulsion preparation and then characterizes the emulsion characteristics after it is pumped through a common rail system. It then goes on to examine the spray of the pumped emulsions (10% water concentration at injection pressures of 500, 1000, and 1500 bar) into a high-temperature gas environment and the puffing and/or micro-explosion of the droplets. A specifically developed image processing system algorithm was used to process the captured images of the droplets.

## 2. Experimental Method

### 2.1. Emulsion Preparation, Stability, and Physical Properties

A Span 80 (a lipophilic surfactant) with a hydrophilic-lipophilic balance (HLB) of 4.3 was used as the emulsifying agent to prepare 10% ( $v/v$ ) water in diesel emulsion. A gravitational method [35–37] was used to characterize the stability of the emulsion. For this purpose, a mechanical stirrer running at 1000 rpm for 10 min was used to blend the emulsion, which was then stored in cylindrical tubs as shown in Figure 1. Then, the de-emulsifications of the blends were recorded at different times and the separation of the layer. For the first 4 h the emulsion was stable; it then exhibited some de-emulsification after this time. However, a complete separation was observed after 3 days. In the current work, the emulsions were promptly (less than 15 min) induced into the fuel tank after their preparation and run through the common rail system to avoid this phase separation.

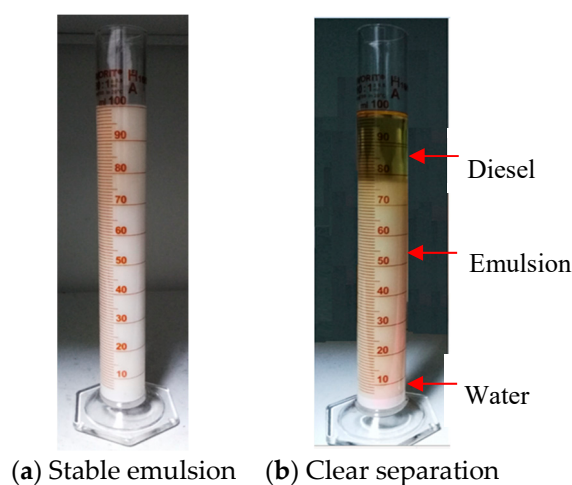


**Figure 1.** Picture of water-in-diesel emulsion at 10% water content showing the emulsions before separation (a) and with the layers of separation (b).

### 2.2. Physical Properties

The viscosity and density of the neat diesel and emulsions were measured using an Anton Paar viscometer (Lovis 2000M) (Anton Paar, Graz, Austria) and an Anton Paar density meter (DMA 4500M) (Anton Paar, Graz, Austria), respectively. An isoperibol calorimeter (Leco AC-350) (AC-350, Leco, Graz, Austria) was used to measure the calorific value, and the surface tension was measured using the pendant drop method (Data Physics OCA 15EC). The properties of all fuels tested are shown in Table 1.

**Table 1.** Properties of neat diesel and water-in-diesel emulsions.

Water Content (% (v/v))	Density at 25 °C (kg/m <sup>3</sup> )	Viscosity at 40 °C (mm <sup>2</sup> /s)	Calorific Value (MJ/kg)	Surface Tension at 25 °C (N.m)
0 (neat diesel)	825	3.21	43.20	27.1
10	855	9.53	39.15	23.9

### 2.3. Fuel Injection System

An electronic fuel injection system (common rail) was used to spray and collect the injected samples, in order to characterize the emulsion's size distribution. The complete details for the setup, including the control of the injector opening and duration, can be found in the authors' previous work [32,35].

### 2.4. Image Acquisition and Analysis

The dispersed water droplet distribution was captured by using a digital microscope (Olympus BX51) with a magnification of 50 times and depth of field of 10  $\mu\text{m}$ . A purpose-developed image processing algorithm built in MATLAB was used to analyze all the raw images. This algorithm automatically detects and measures the dispersed droplet size and number. The image processing sequence is discussed in detail in our previous work [32,35]. The equivalent diameter of each detected droplet was calculated based on the droplet's area. This equivalent diameter was used to plot the graphs in Section 3.

### 2.5. Optical System

Experiments were conducted using an optically accessible constant-volume chamber (Figure 2). This chamber was of a cylindrical shape, offering the visualization of the full spray and spray droplets. The chamber was constructed from stainless steel including a cylindrical enclosure, two flanges, and two optical windows for flow visualization. A ceramic electric heater was mounted on the cylinder wall to heat the chamber. A micro pump controller (Micro 4) with a needle diameter of 0.3 mm was used to generate the spray droplets. The Micro 4 provided flexibility in controlling the injection time, injection duration, and the amount of fuel to be injected, while producing droplets that could be easily observed. The needle was located in its position after the desired temperature was reached in order to avoid heat transfer to the needle tip which may affect the spray droplets before they were dispensed. Two thermocouples (K-type) were used to measure the temperatures on the surfaces of the chamber as well as the gas temperature located at the center inside the chamber before the injection. The temperature distribution inside the chamber was 730 K while the chamber walls were at 800 K due to heat transfer from the walls to the ambient gas.

### 2.6. Processing and Analysis of Spray Droplets

A shadowgraph imaging system was developed to acquire detailed records of the spray droplets. It consisted of a high-speed video camera (Phantom Miro M310) (Wayne, NJ, USA) coupled with a long-distance microscope (Infinity K2) (Boulder, CO, USA) and zoom lens (CF1 objective) (Boulder, CO, USA). A Multi LED (LT-V8-15) (Tokyo, Japan) was used for the illumination. The experiments were performed with a resolution of  $256 \times 800$  pixel (0.0185 mm/pixel), frame rates of 12,000 frames per second (fps), and exposure time of 2  $\mu\text{s}$ . The minimum spray droplets measured were 20  $\mu\text{m}$ , and smaller sizes were not included due to experimental uncertainty. Droplets were not ignited during these experiments. All raw images were then analyzed using a specifically developed image processing algorithm to automatically detect the spray droplets and measure their sizes. The image processing sequence was as follows: the raw image was converted to a binary format with a threshold setting, then edge detection, filling holes of droplets, watershed to separate connected droplets, and, finally, segmentation of the image were applied. The detected droplet diameter was calculated based on the droplet's area. To include a sufficient number of droplets, each sample was repeated several times under the same experimental conditions.

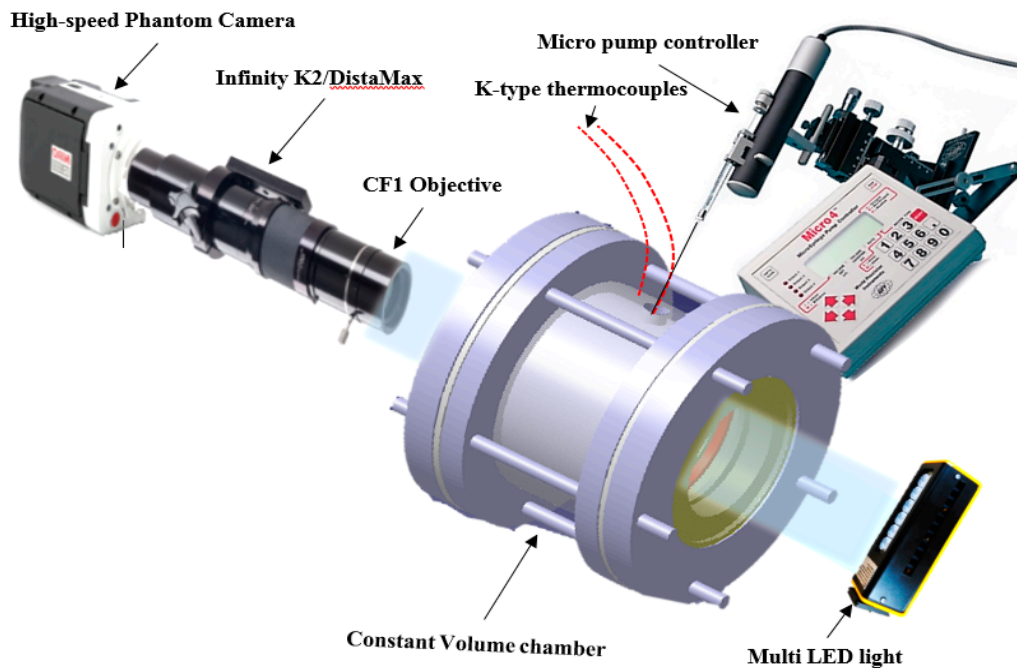


**Figure 2.** Schematic of the combustion chamber showing the optical accesses and the long-distance microscope imaging system. The Multi LED light used to provide the back illumination.

### 3. Results and Discussion

Based on the evidence that the injector nozzle shifts the size distribution of the dispersed phase towards smaller droplet sizes (discussed in the previous works [32,35]), only samples after the injector were used in each experiment.

#### 3.1. The Effect of Injector Shearing on Droplet Size Distribution

After the injection system ran, we collected three samples at injection pressures of 500, 1000, and 1500 bar of 10% (*v/v*) emulsion blend. Figure 3 shows the distribution of the dispersed water droplets in the fuel tank (fresh emulsion) and after injector at pressures of 500 bar (A), 1000 bar (B), and 1500 bar (C). It can be clearly noticed that the size and number of the dispersed water droplets were affected significantly by the shear force in the injector nozzle, as expected from our previous work [32]. An increase in injection pressure led to the breakup of the dispersed droplet size and, thereby, to decreases in their sizes.

To ensure that the water concentration in the emulsion had reduced, a mixing model was used to calculate the water content for each blend based on density measurement. Figure 4 shows the water concentration at 10% (*v/v*) at different injection pressures (500, 1000, and 1500 bar); this indicates that with the increase of injection pressure i.e., 500, 1000, and 1500 bar, the water concentration was reduced to 9.4%, 9.2%, and 8.7% respectively, as expected. This can be attributed to the water lost or evaporated during the injection with the intensive shear in the injector nozzle. It can therefore be confirmed that the emulsions in the fuel tank can change significantly with time [32]. The evaporated water during the injection reduces the adiabatic flame temperature and therefore reduces the NO<sub>x</sub> emissions. Water dissociation can form hydroxyl radicals during combustion and therefore reduce soot emissions [8]. This finding broadly supports the work of other studies in the area of micro-explosion linking the single-droplet experiments [36] with engine performance and emissions [6]. Therefore, the single-droplet experiments do not accurately simulate the dispersed water droplets and water concentration. Next, only the emulsions after the injection equipment were considered to examine their effect on the secondary atomization.

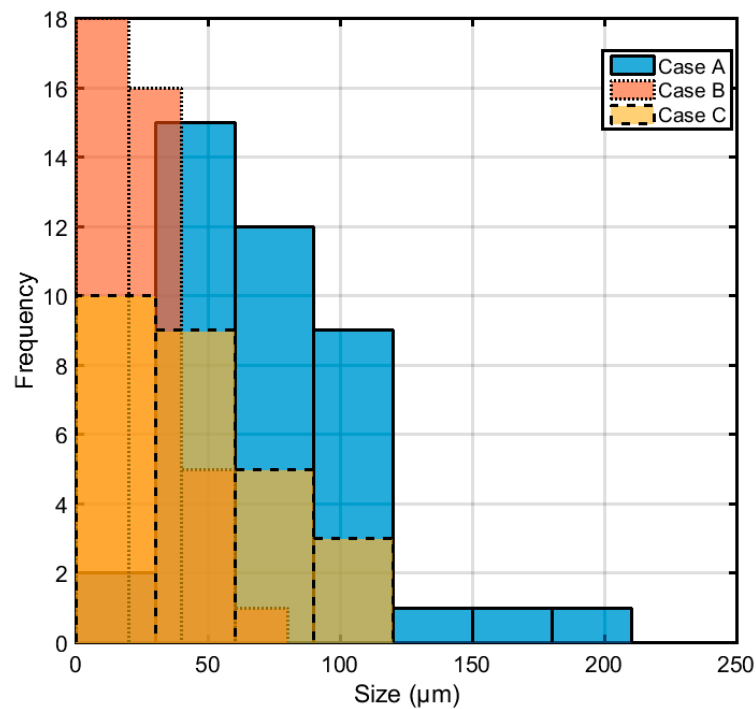


**Figure 3.** Histogram of the emulsions used for the experiments made at 10% water in fuel tank (Fresh) and Cases A, B, and C after the fuel equipment at different injection pressures of 500, 1000, and 1500 bar, respectively.

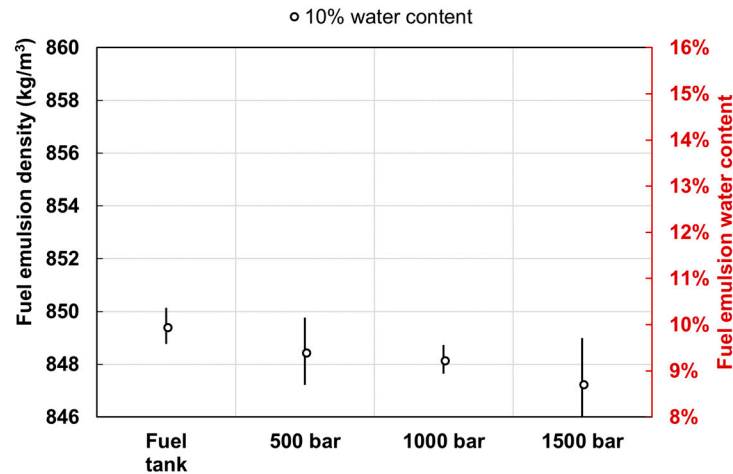


**Figure 4.** The density measurement of an emulsion made with 10% water content at different injection pressures. The density reduced with the increase of injection pressure as the result of a reduction in the water concentration of the emulsion.

### 3.2. Spray Droplet Puffing and Micro-Explosion Phenomena

The emulsion samples were collected after injection at 500, 1000, and 1500 bar. These samples were then injected into the combustion chamber using the microsyringe, into an environment with a gas temperature of 723 K. The images in Figure 5a show the spray droplet behavior at 1.25 ms and 2.4 ms after injection while Figure 5b focuses on magnified droplets at different times. The images reveal that, even for very fine droplets, water vapor erupts from the droplets, resulting in secondary atomization. As shown in Figure 5a, most of the spray droplets are nonspherical near the injector



nozzle and do not break up due to the high surface tension [37]. As can be seen in Figure 5b Case (I), the droplet became spherical during water evaporation, and puffing occurred at 3.5 ms prior to evaporation. Figure 5b Case (II) shows that puffing occurred twice for the same droplet, which is thought to be due to the high water concentration. The distributions of water inside the droplets were not always the same [38]. A complete micro-explosion can be seen clearly in Case (III) with a droplet diameter of 100  $\mu\text{m}$  at 6.12 ms. However, almost all smaller droplets burst instantaneously, and very fine secondary droplets were produced and evaporated. Qualitatively, a similar behavior was observed in Case (IV) with increasing waiting time of 7.34 ms. Interestingly, in Case (V), the ejected droplet was observed to undergo further micro-explosion. These results confirm that residence time is a significant factor for micro-explosion outcomes. Longer waiting times increase the probability of micro-explosion.

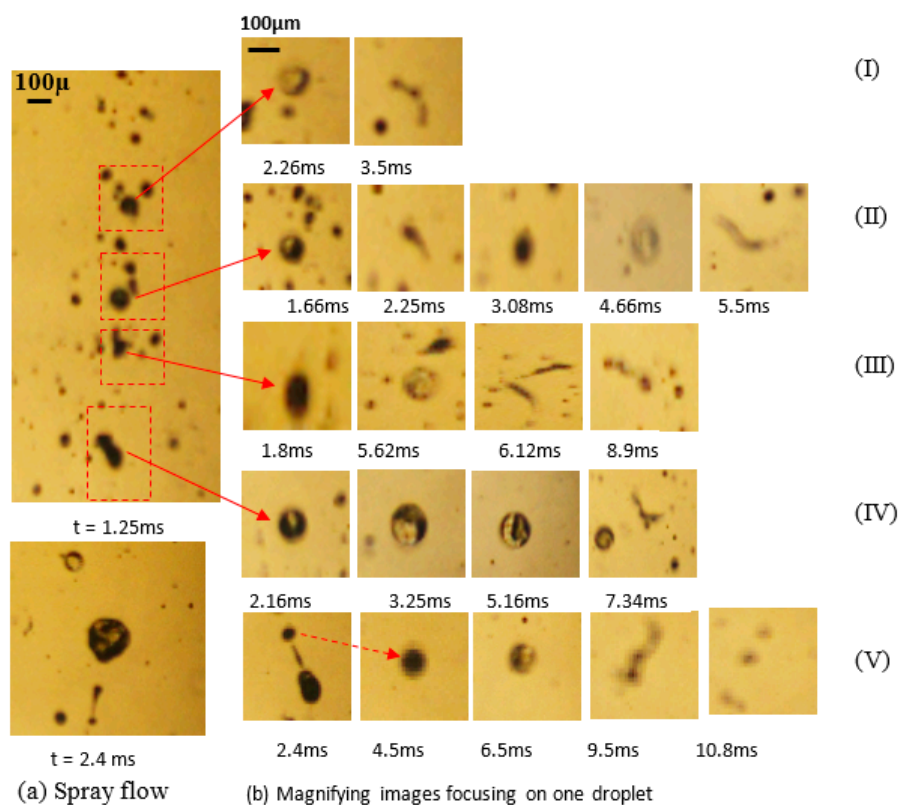


**Figure 5.** (a) Sequences of spray flow droplets of 10% water concentration at 723 K for Sample A, showing puffing and micro-explosion; (b) shows the magnified droplet micro-explosion phenomena.

### 3.3. Spray Droplets Size Versus Time to Puffing

In this section, the dynamics of micro-explosion and puffing were tracked for a falling emulsified fuel droplet and an attempt was made to understand the mechanism and the stages involved in the secondary atomization. In all cases, although the droplets' evaporation progressed, their size gradually increased as the spray moved downstream (Figure 6). It can therefore be assumed that the rate of droplet thermal expansion due to water evaporation was greater than the droplet shrinkage caused by the evaporation from the droplet. In the first stage ( $t = 0$  to 2 ms) the droplets were nonspherical as they left the microsyringe. The size of the droplets tended to decrease abruptly and followed an oscillatory path. In the second stage ( $t = 2$  to 5 ms), as the droplet stabilized and converged towards sphericity, their size continued to increase due to water evaporating inside the droplet until it reaches the puffing limit, the point where the droplet ebullition occurred. The droplet oscillation decreased as they became more spherical and moved in a straight path. In the third stage ( $t = 5$  to 10 ms), Droplets 1, 3, and 4 underwent puffing, reducing in size and giving birth to satellite droplets. However, Droplet

2 continued to increase in size over time until it reached the puffing limit at a much later stage ( $t = 10$  to  $16$  ms). As the size of the parent emulsion droplet increased, the puffing time also increased as shown by Case 3 and Case 4. However, the physics differs in Case 1 and Case 4 which can be attributed to the dispersed size of the water content within the parent emulsion droplet and the location of the vapor nuclei [21,39]. Again, in Cases 1 and 2, a similar behavior is observed; however, their times to puffing were different although their initial droplet sizes were almost the same. It is also observed that in some cases the droplets tended to grow in size again after puffing, indicating the partial utilization of water dispersed within the parent droplet. This could be because of partial coalescence of dispersed water droplets [32], and, as a result, complete micro-explosion was not observed. In this case, the satellite droplets may have the potential to undergo further puffing. Perhaps the most interesting aspect of this is that the initial and final droplet sizes before puffing will determine the effect of the dispersed water in the parent droplet on the growth of the droplet. Next, we consider the effect of injection pressure on puffing occurrence.

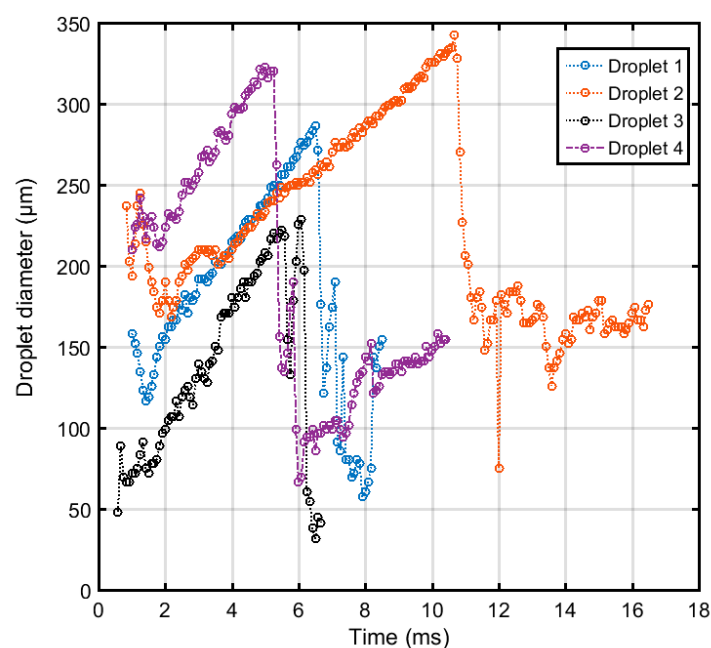


**Figure 6.** Effect of different droplet size on time to puffing of 10% water content sprayed at 1000 bar injection pressure.

### 3.4. Effect of Injection Pressure and Dispersed Water Droplet Size on Droplet Puffing

As discussed earlier, both the size of the dispersed water droplets and the water content in the emulsion droplets are significantly affected by the injection pressure. Therefore, it is expected that the explosive boiling of the dispersed water droplets will be influenced by the injection pressure. By measuring and comparing the initial droplet size and that before puffing, one can estimate the amount of water leaving the droplets [40]. Figure 7 represents the empirical cumulative distribution functions for the initial droplet size and the final droplet size before puffing for emulsions in Cases A, B, and C (Figure 3).

In all cases, the droplet expansion increased with the increase of dispersed water droplet size. The spray initial droplet size was found to be large for the higher water content with larger dispersed size due to higher viscosity. Significant differences were observed in Case C which had the smallest dispersed water droplets. Since coalescence of the dispersed water droplets is not expected to take place due to the very short residence time in the spray, the initial dispersed water droplet size will be the major factor influencing secondary atomization. This finding suggests that increasing the injection pressure will reduce the intensity of micro-explosion due to evaporation and the decrease of dispersed water in



the spray. With large dispersed water droplet size, the boiling rate increases and therefore enhances the secondary atomization. These findings are consistent with those of Mura et al. [28], who observed that droplet growth increased with the increase of dispersed water droplet size. Also, Volkov et al. [20] argued that evaporation of droplets flowing in a high temperature decelerated with the increase of water concentration. This behavior was found to be enhanced when the initial droplet size increased.

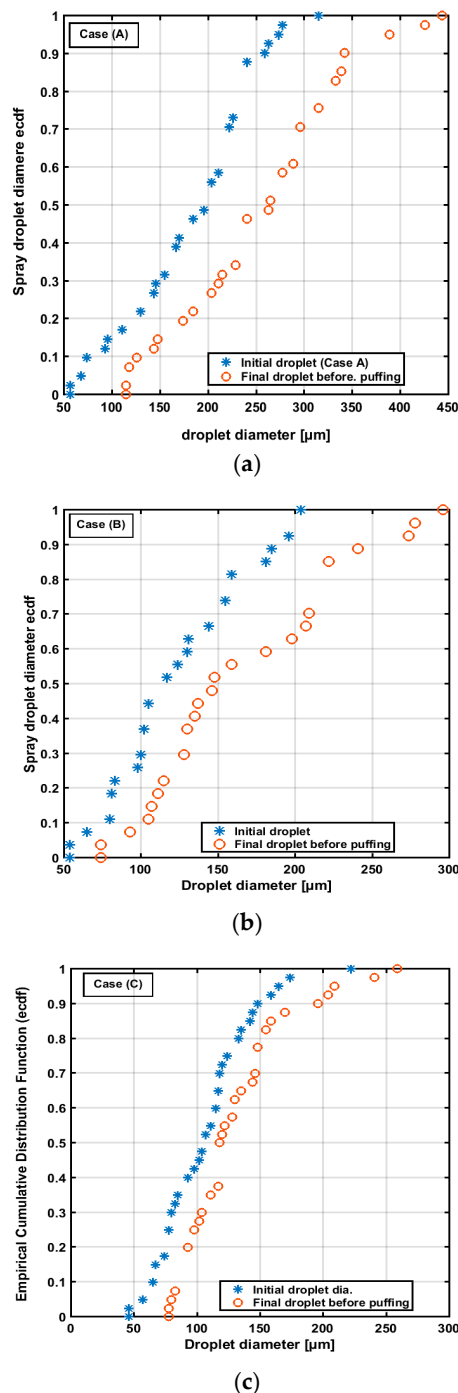


**Figure 7.** The empirical cumulative distribution function (ECDF) shows the spray initial droplet size versus the droplet expansion before puffing for different injection pressures: (a) Case A (500 bar), (b) Case B (1000 bar) and (c) Case C (1500 bar). As the dispersed water droplet size decreased via the injection pressure, the droplet expansion was decreased.

To go further on the effect of dispersed water droplet size on the puffing behavior, the time duration between the initial and final droplet before puffing are presented in Figure 8 using the empirical cumulative distribution function (ECDF). With the decrease of dispersed water droplet size due to injection pressure, the amount of dispersed water decreased and, hence, the time to puffing increased. These results indicate that higher injection pressures have a negative effect on secondary atomization. With the higher injection pressure, some spray droplets may not include sufficiently large dispersed water droplets to initiate puffing.

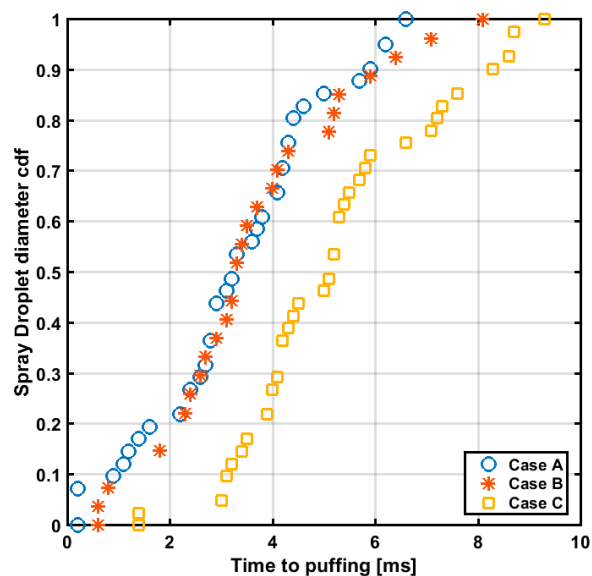


**Figure 8.** The empirical cumulative distribution function of dispersed water droplet size after the injection at 500 (A), 1000 (B), and 1500 bar (C) injection pressure versus time duration to puffing. As the injection pressure increased, the time to puffing was delayed.

#### 4. Conclusions

We investigated the effect of fuel injection pressure on puffing and micro-explosion of water-in-diesel emulsion under elevated gas temperatures. To determine the effect of a common rail system on micro-explosion, we simulated the spray samples at different injection pressures and measured the evolution of the number and size distributions of the dispersed phase. Our major findings from this study are summarized as follows:

1. We found that the emulsion properties (dispersed droplet size and numbers) change significantly after the nozzle's orifices, as expected; the water concentration reduced after the injection due to rapid evaporation caused by high pressure and temperature in the common rail [32].
2. With the increase of injection pressure, puffing was delayed due to reduction in dispersed water droplet size and water content in the emulsion.
3. In the experiment, puffing and micro-explosion were observed in small droplets ( $>50\ \mu\text{m}$ ) after a clear transparent region. Since coalescence of the dispersed water droplets is not expected to take place due to the very short residence time in the spray, complete micro-explosion was not observed.
4. The droplet time to puffing was found to be related more to the dispersed droplet size and water content in the droplet rather than to the spray droplet size.

This investigation suggested that the injection equipment influences secondary atomization via the dispersed water droplets and evaporation of water during the spray. The occurrence of micro-explosion during the spray will depend not only on spray droplet size but also on the coalescence of the dispersed water droplets. These findings may support the hypothesis of using unstable emulsions [41].

**Author Contributions:** The work was supervised by M.R.H., A.R.A.A., C.C. and M.B.B. The experiments and data analysis were carried out by M.A.I., M.E.-A., Z.N., E.Z.Z.A. and F.

**Funding:** This research was supported by the Malaysia's Grants FRGS (Ref: FRGS/1/2017/TK10/UTP/01/2).

**Acknowledgments:** The authors would like to acknowledge the support given by the Universiti Teknologi PETRONAS to the Centre for Automotive Research and Electric Mobility (CAREM) in performing this research.

**Conflicts of Interest:** The authors declare no conflict of interest.

## References

1. Kannan, K.; Udayakumar, M. NO<sub>x</sub> and HC emission control using water emulsified diesel in single cylinder diesel engine. *J. Eng. Appl. Sci.* **2009**, *4*, 59–62.
2. Tauzia, X.; Maiboom, A.; Shah, S.R. Experimental study of inlet manifold water injection on combustion and emissions of an automotive direct injection Diesel engine. *Energy* **2010**, *35*, 3628–3639. [[CrossRef](#)]
3. Bedford, F.; Rutland, C.; Dittrich, P.; Raab, A.; Wirbeleit, F. Effects of direct water injection on di diesel engine combustion. *SAE Tech. Pap.* **2000**, *1*, 2938. [[CrossRef](#)]
4. Arabaci, E.; İcingür, Y.; Solmaz, H.; Uyumaz, A.; Yilmaz, E. Experimental investigation of the effects of direct water injection parameters on engine performance in a six-stroke engine. *Energy Convers. Manag.* **2015**, *98*, 89–97. [[CrossRef](#)]
5. Farfaletti, A.; Astorga, C.; Martini, G.; Manfredi, U.; Mueller, A.; Rey, M.; De Santi, G.; Krasenbrink, A.; Larsen, B.R. Effect of water/fuel emulsions and a cerium-based combustion improver additive on HD and LD diesel exhaust emissions. *Environ. Sci. Technol.* **2005**, *39*, 6792–6799. [[CrossRef](#)] [[PubMed](#)]
6. Attia, A.M.A.; Kulchitskiy, A.R. Influence of the structure of water-in-fuel emulsion on diesel engine performance. *Fuel* **2014**, *116*, 703–708. [[CrossRef](#)]
7. Lv, G.; Wang, F.; Cai, W.; Li, H.; Zhang, X. Influences of addition of hydrophilic surfactants on the W/O emulsions stabilized by lipophilic surfactants. *Colloids Surf. A Physicochem. Eng. Asp.* **2014**, *457*, 441–448. [[CrossRef](#)]
8. Wang, Z.; Shi, S.; Huang, S.; Tang, J.; Du, T.; Cheng, X.; Huang, R.; Chen, J.-Y. Effects of water content on evaporation and combustion characteristics of water emulsified diesel spray. *Appl. Energy* **2018**, *226*, 397–407. [[CrossRef](#)]
9. Wang, Z.; Wu, S.; Huang, Y.; Huang, S.; Shi, S.; Cheng, X.; Huang, R. Experimental investigation on spray, evaporation and combustion characteristics of ethanol-diesel, water-emulsified diesel and neat diesel fuels. *Fuel* **2018**, *231*, 438–448. [[CrossRef](#)]
10. Huo, M.; Lin, S.; Liu, H.; Lee, C.F. Study on the spray and combustion characteristics of water-emulsified diesel. *Fuel* **2014**, *123*, 218–229. [[CrossRef](#)]
11. Yang, W.M.; An, H.; Chou, S.K.; Chua, K.J.; Mohan, B.; Sivasankaralingam, V.; Raman, V.; Maghbouli, A.; Li, J. Impact of emulsion fuel with nano-organic additives on the performance of diesel engine. *Appl. Energy* **2013**, *112*, 1206–1212. [[CrossRef](#)]
12. Park, J.W.; Huh, K.Y.; Park, K.H. Experimental study on the combustion characteristics of emulsified diesel in a rcem. *Proc. Inst. Mech. Eng. Part D: J. Automob. Eng.* **2000**, *214*, 579–586. [[CrossRef](#)]
13. Park, S.; Woo, S.; Kim, H.; Lee, K. The characteristic of spray using diesel water emulsified fuel in a diesel engine. *Appl. Energy* **2016**, *176*, 209–220. [[CrossRef](#)]
14. Niioka, T.; Sato, J. Combustion and microexplosion behavior of miscible fuel droplets under high pressure. *Symp. Combust.* **1988**, *21*, 625–631. [[CrossRef](#)]
15. Ochoterena, R.; Lif, A.; Nydén, M.; Andersson, S.; Denbratt, I. Optical studies of spray development and combustion of water-in-diesel emulsion and microemulsion fuels. *Fuel* **2010**, *89*, 122–132. [[CrossRef](#)]
16. Zhu, M.; Zhang, Z.; Zhang, Y.; Liu, P.; Zhang, D. An experimental investigation into the ignition and combustion characteristics of single droplets of biochar water slurry fuels in air. *Appl. Energy* **2017**, *185*, 2160–2167. [[CrossRef](#)]
17. Kichatov, B.; Korshunov, A.; Kiverin, A.; Saveliev, A. The role of explosive boiling in the process of foamed emulsion combustion. *Int. J. Heat Mass Transf.* **2018**, *119*, 199–207. [[CrossRef](#)]
18. Tarlet, D.; Mura, E.; Josset, C.; Bellettre, J.; Allouis, C.; Massoli, P. Distribution of thermal energy of child-droplets issued from an optimal micro-explosion. *Int. J. Heat Mass Transf.* **2014**, *77*, 1043–1054. [[CrossRef](#)]
19. Law, C.K.; Lee, C.H.; Srinivasan, N. Combustion characteristics of water-in-oil emulsion droplets. *Combust. Flame* **1980**, *37*, 125–143. [[CrossRef](#)]

20. Volkov, R.S.; Kuznetsov, G.V.; Strizhak, P.A. Influence of droplet concentration on evaporation in a high-temperature gas. *Int. J. Heat Mass Transf.* **2016**, *96*, 20–28. [\[CrossRef\]](#)
21. Shinjo, J.; Xia, J.; Ganippa, L.C.; Megaritis, A. Physics of puffing and microexplosion of emulsion fuel droplets. *Phys. Fluids* **2014**, *26*, 103302. [\[CrossRef\]](#)
22. Ismael, M.A.; Heikal, M.R.; Aziz, A.R.A.; Crua, C. An Overview of Experimental Techniques of the Investigation of Water-Diesel Emulsion Characteristics Droplets Micro-Explosion. *ARPN J. Eng. Appl. Sci.* **2016**, *11*, 11975–11981.
23. Tarlet, D.; Bellettre, J.; Tazerout, M.; Rahmouni, C. Prediction of micro-explosion delay of emulsified fuel droplets. *Int. J. Therm. Sci.* **2009**, *48*, 449–460. [\[CrossRef\]](#)
24. Mura, E.; Calabria, R.; Califano, V.; Massoli, P.; Bellettre, J. Emulsion droplet micro-explosion: Analysis of two experimental approaches. *Exp. Therm. Fluid Sci.* **2014**, *56*, 69–74. [\[CrossRef\]](#)
25. Khan, M.Y.; Karim, Z.A.A.; Aziz, A.R.A.; Morgan, R.; Crua, C. Puffing and Microexplosion Behavior of Water in Pure Diesel Emulsion Droplets During Leidenfrost Effect Puffing and Microexplosion Behavior of Water in Pure Diesel. *Combust. Sci. Technol.* **2017**, *189*, 1186–1197. [\[CrossRef\]](#)
26. Califano, V.; Calabria, R.; Massoli, P. Experimental evaluation of the effect of emulsion stability on micro-explosion phenomena for water-in-oil emulsions. *Fuel* **2014**, *117*, 87–94. [\[CrossRef\]](#)
27. Kimoto, K.; Owashi, Y.; Omae, Y. The vaporizing behavior of the fuel droplet of water-in-oil emulsion on the hot surface. *Bull. JSME* **1986**, *258*, 4247–4255. [\[CrossRef\]](#)
28. Mura, E.; Massoli, P.; Josset, C.; Loubar, K.; Bellettre, J. Study of the micro-explosion temperature of water in oil emulsion droplets during the Leidenfrost effect. *Exp. Therm. Fluid Sci.* **2012**, *43*, 63–70. [\[CrossRef\]](#)
29. Mura, E.; Josset, C.; Loubar, K.; Huchet, G.; Bellettre, J. Effect of dispersed water droplet size in microexplosion phenomenon for water in oil emulsion. *At. Sprays* **2010**, *20*, 791–799. [\[CrossRef\]](#)
30. Sechremeli, D.; Stampouli, A.; Stamatoudis, M. Comparison of mean drop sizes and drop size distributions in agitated liquid-liquid dispersions produced by disk and open type impellers. *Chem. Eng. J.* **2006**, *117*, 117–122. [\[CrossRef\]](#)
31. Watanabe, H.; Okazaki, K. Visualization of secondary atomization in emulsified-fuel spray flow by shadow imaging. *Proc. Combust. Inst.* **2013**, *34*, 1651–1658. [\[CrossRef\]](#)
32. Ismael, M.A.; Heikal, M.R.; Aziz, A.R.A.; Syah, F.; Crua, C. The effect of fuel injection equipment on the dispersed phase of water-in-diesel emulsions. *Appl. Energy* **2018**, *222*, 762–771. [\[CrossRef\]](#)
33. Jackson, G.S.; Avedisian, C.T. Combustion of unsupported water-in-n-heptane emulsion droplets in a convection-free environment. *Int. J. Heat Mass Transf.* **1998**, *41*, 2503–2515. [\[CrossRef\]](#)
34. Kim, H.; Won, J.; Baek, S.W. Evaporation of a single emulsion fuel droplet in elevated temperature and pressure conditions. *Fuel* **2018**, *226*, 172–180. [\[CrossRef\]](#)
35. Ismael, M.A.; Heikal, M.R.; Aziz, A.A.; Crua, C. The Effect of Fuel Injection Equipment of Water-In-Diesel Emulsions on Micro-Explosion Behaviour. *Energies* **2018**, *11*, 1650. [\[CrossRef\]](#)
36. Khan, M.Y.; Karim, Z.A.A.; Aziz, A.R.A.; Tan, I.M. A case study on the influence of selected parameters on microexplosion behavior of water in biodiesel emulsion droplets. *J. Energy Resour. Technol.* **2017**, *139*, 1–10.
37. Agrawal, M.; Premkata, A.R.; Tripathi, M.K.; Karri, B.; Sahu, K.C. Nonspherical liquid droplet falling in air. *Phys. Rev. E* **2017**, *95*, 033111. [\[CrossRef\]](#) [\[PubMed\]](#)
38. Khan, M.Y.; Abdul Karim, Z.A.; Aziz, A.R.A.; Tan, I.M. Experimental Investigation of Microexplosion Occurrence in Water in Diesel Emulsion Droplets during the Leidenfrost Effect. *Energy & Fuels* **2014**, *28*, 7079–7084.
39. Lasheas, J.C.; Yap, L.T.; Dryer, F.L. Effect of the ambient pressure on the explosive burning of emulsified and multicomponent fuel droplets. *Symp. Combust.* **1985**, *20*, 1761–1772. [\[CrossRef\]](#)
40. Kadota, T.; Tanaka, H.; Segawa, D.; Nakaya, S.; Yamasaki, H. Microexplosion of an emulsion droplet during Leidenfrost burning. *Proc. Combust. Inst.* **2007**, *31*, 2125–2131. [\[CrossRef\]](#)
41. Ithnin, A.M.; Yahya, W.J.; Ahmad, M.A.; Ramlan, N.A.; Abdul Kadir, H.; Sidik, N.A.C.; Koga, T. Emulsifier-free water-in-diesel emulsion fuel: Its stability behaviour, engine performance and exhaust emission. *Fuel* **2018**, *215*, 454–462. [\[CrossRef\]](#)

